Eur. J. Biochem. 204, 779–782 (1992)

Mössbauer characterization of the tetraheme cytochrome c_3 from *Desulfovibrio baculatus* (DSM 1743)

Spectral deconvolution of the heme components

Natarajan RAVI[1], Isabel MOURA[2], Cristina COSTA[2], Miguel TEIXEIRA[2], Jean LeGALL[3], José J. G. MOURA[2] and Boi Hanh HUYNH[1]

[1] Department of Physics, Emory University, Atlanta, USA
[2] Centro de Tecnologia Química e Biológica and Universidade Nova de Lisboa, Oeiras, Portugal
[3] Department of Biochemistry, University of Georgia, Athens, USA

(Received October 7/November 29, 1991) – EJB 91 1332

Mössbauer spectroscopy was used to study the tetraheme cytochrome c_3 from *Desulfovibrio baculatus* (DSM 1743). Samples with different degrees of reduction were prepared using a redox-titration technique. In the reduced cytochrome c_3, all four hemes are reduced and exhibit diamagnetic Mössbauer spectra typical for low-spin ferrous hemes ($S = 0$). In the oxidized protein, the hemes are low-spin ferric ($S = 1/2$) and exhibit overlapping magnetic Mössbauer spectra. A method of differential spectroscopy was applied to deconvolute the four overlapping heme spectra and a crystal-field model was used for data analysis. Characteristic Mössbauer spectral components for each heme group are obtained. Hyperfine and crystal-field parameters for all four hemes are determined from these deconvoluted spectra.

Cytochrome c_3 is a class of small proteins (molecular mass $\approx$ 13 kDa) found in sulfate-reducing bacteria [1]. Each molecule contains four hemes and each heme is bound to the polypeptide chain by two thioether linkages. In addition, each heme iron is coordinated to two histidine residues as axial ligands. The three-dimensional molecular structure for cytochrome c_3 has been determined by X-ray crystallography for the species *Desulfovibrio vulgaris* (Miyazaki) [2], *D. baculatus* (Norway 4) [3, 4] and *Desulfovibrio gigas* [5]. It is found that the relative positions and orientations for the four hemes in these cytochromes are quite similar despite the lack of homology in their amino-acid sequences. Furthermore, the four hemes are found to be situated in different protein environments and have different axial-ligand orientations.

In the as-isolated protein, all four hemes are oxidized and exhibit characteristic low-spin ferric EPR signals, resulting in a poorly resolved spectrum [6–10]. Depending on the organism, the maximum g-values (g_{max}) for the four hemes vary between 2.7–3.4. The middle g-values (g_{mid}) are observed around 2.1–2.3. In general, only one or two minimum g-values (g_{min}) are detected while the others are not observable due to g-strain broadening. Because of the poor resolution, assignment of individual heme EPR signals is difficult. Nevertheless, potentiometric titrations monitored by EPR have been performed on cytochrome c_3 isolated from many different species and mid-point redox potentials for the heme groups have been determined [6–10]. Even though the four hemes are of the same type, their mid-point redox potentials are different and depending on the species, the mid-point potentials of the four hemes can vary from -360 to -70 mV. Furthermore, these EPR redox titration studies, as well as detailed proton-NMR studies on cytochrome c_3 from *D. gigas* [11], *D. vulgaris* (Hildenborough) [12] and *D. vulgaris* (Miyazaki) [13, 14] have established that the heme mid-point redox potential can be influenced by the oxidation states of the other surrounding hemes and that this heme-heme interaction can change the redox potential by as much as 60 mV.

In this manuscript, we report a Mössbauer study of the tetraheme cytochrome c_3 from *D. baculatus* (DSM 1743). Samples with different degrees of reduction were prepared using a redox-titration technique and the samples were examined by Mössbauer spectroscopy. The method of differential spectroscopy was used to resolve the overlapping heme spectra. Characteristic Mössbauer spectra, hyperfine parameters and crystal-field parameters were obtained for all four hemes.

MATERIALS AND METHODS

^{57}Fe-enriched cells of *D. baculatus* (DSM 1743) were grown in a lactate-sulfate medium as previously described [15]. The medium contained 0.5 mg ^{57}Fe/l (95% enrichment, New England Nuclear). Cells from a 400-l fermenter were harvested by centrifugation at the end of the exponential growth phase and stored at -80 °C. Cytochrome c_3 was purified following the procedures described by G. Fauque [16]. The Mössbauer samples were poised at different redox potentials in an anaerobic vessel similar to that described by Dutton [17]. The cytochrome c_3 solution contained 0.83 mM proteins in 0.1 M Tris/HCl, pH 8.1. The oxidation reduction titrations were carried out at 25 °C with the following mediators at a final concentration of 10 μM: phenosaphranine, benzylviologen, methylviologen and 2-hydroxy-(1,4)-naphtoquinone. The potential was adjusted by the addition of small amounts of dithionite or ferricyanide solution. After equilibration at a chosen redox potential, samples were transferred into a

Correspondence to B. H. Huynh, Department of Physics, 1510 Clifton Road, NE, Emory University, Atlanta, GA, USA 30322

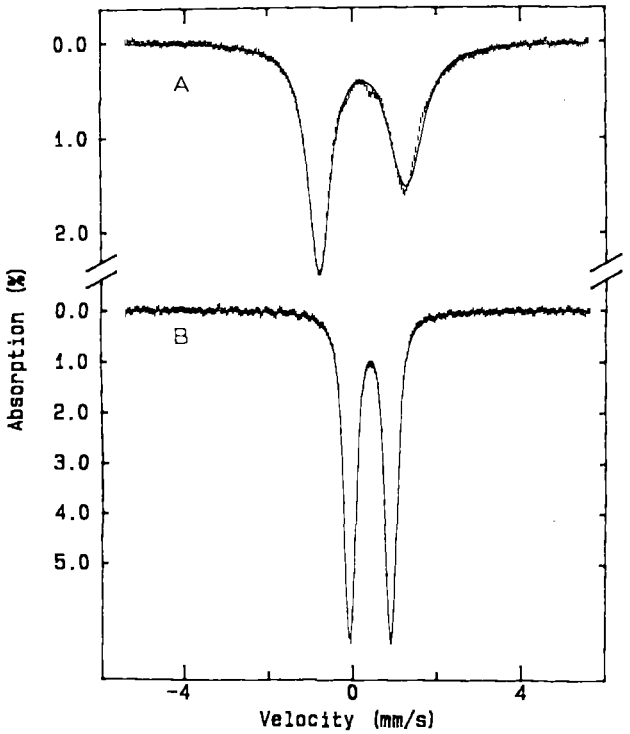

Fig. 1. 100 K Mössbauer spectra of cytochrome c_3 from *D. baculatus* (DSM 1743) poised at +250 mV (A) and −450 mV (B). The solid lines are least-squares fits to the data assuming four equal intensity quadrupole doublets (see text).

Mössbauer cell and an EPR tube simultaneously and frozen immediately in liquid nitrogen. Both the Mössbauer cell and the EPR tube were attached to the redox vessel and were detached only after the samples were frozen. Samples at +250 mV, −210 mV, −300 mV, −340 mV and −450 mV were prepared for this study. These potentials are quoted versus a normal hydrogen electrode and are chosen to maximize the spectral differences based on our earlier EPR titration study [6] which yielded the following mid-point redox potentials for the four hemes: −70 mV, −280 mV, −300 mV and −355 mV. The EPR samples were prepared as controls to ensure that proper redox states were reached.

Standard transmission Mössbauer measurements were made with a 50 mCi ^{57}Co(Rh) γ-ray source driven by a Doppler velocity transducer operating at the constant acceleration mode. The velocity scale was calibrated using a room-temperature spectra of a metallic iron foil and the zero velocity is referred to the centroid of these spectra. EPR measurements were performed on a Bruker ER 200-SRC spectrometer equipped with an Oxford Instrument continuous flow cryostat.

RESULTS

Fig. 1 shows the Mössbauer spectra of cytochrome c_3 from *D. baculatus* (DSM 1743) poised at +250 mV and −450 mV. The data were recorded at 100 K in the absence of a magnetic field. For the sample poised at the most positive potential (+250 mV), all four hemes are in their oxidized form and the sample exhibits a broad quadrupole doublet (spectrum A). The line widths of the absorption lines are broader than that expected for a single iron site, suggesting that the spectrum is a superposition of different doublets arising from the four different heme groups. (The line width of the high-energy lines, 0.80 mm/s, obtained from the least-squares fit for the four unresolved doublets is much broader than that of the low-energy lines, 0.60 mm/s. This phenomenon is generally observed for a paramagnetic system if the electronic relaxation rate is fast but not too fast in comparison with the nuclear precession rate $\approx 10^7\ s^{-1}$). Similarly, a single but broad quadrupole doublet (spectrum B) is also observed for the sample poised at the most negative potential (−450 mV) where the hemes are reduced. Both spectra can be least-squares fitted with four equal-intensity quadrupole doublets. Since these doublets are unresolved, we report here the average parameters obtained from the least squares fits: $\Delta E_Q = 2.06 \pm 0.23$ mm/s, $\delta = 0.24 \pm 0.05$ mm/s for the oxidized sample and $\Delta E_Q = 0.98 \pm 0.15$ mm/s, $\delta = 0.43 \pm 0.01$ mm/s for the reduced sample. The uncertainties indicate the variations obtained for the four doublets of the corresponding sample. These parameters are characteristics for low-spin ferric ($S = 1/2$) and low-spin ferrous ($S = 0$) heme compounds, respectively. Spectra of samples poised at intermediate potentials are superpositions of these oxidized and reduced doublets with varying intensity ratios (data not shown), indicating the different degrees of reduction of the samples. Using spectra A and B as references for fully oxidized and fully reduced proteins, respectively, the percentages of reduction for the samples can be accurately estimated. They are (23 ± 3) %, (50 ± 5) % and (65 ± 5) % for the −210 mV, −300 mV and −340 mV samples, respectively. These results agree reasonably well with an EPR redox titration study reported previously [6] and are pertinent for the analysis of the corresponding low temperature Mössbauer spectra.

Fig. 2 shows the 4.2 K Mössbauer spectra for the fully oxidized *D. baculatus* cytochrome c_3 recorded in the presence of a 50 mT field (spectrum A) and a 8 T field (spectrum B). The fields are applied parallel to the direction of the γ-beam. At such a low temperature, low-spin ferric heme proteins generally exhibit a magnetically split Mössbauer spectrum with hyperfine features. As expected, in the presence of a magnetic field, *D. baculatus* cytochrome c_3 shows magnetic spectra with resolved hyperfine features. However, in the absence of a magnetic field, the protein shows a spectrum consisting of largely a quadrupole doublet (spectrum not shown), suggesting that the hemes are weakly coupled magnetically. The strength of this coupling is relatively weak, because it can be broken by the application of a field of 50 mT (corresponding to approximately $4.7 \times 10^{-2}\ cm^{-1}$ in energy for an $S = 1/2$ system). This weak coupling is probably dipolar in nature and through space as expected from the close proximity of the hemes.

In order to characterize the four low-spin ferric hemes, we analyzed the magnetic spectra of the oxidized cytochrome c_3 in detail. The spectra are treated as superpositions of four spectral components corresponding to the four low-spin ferric hemes and each component is analyzed by the following $S = 1/2$ spin Hamiltonian:

$$\hat{H} = \beta \vec{S} \cdot \tilde{g} \cdot \vec{H} + \vec{S} \cdot \tilde{A} \cdot \vec{I} + \frac{eQV_{zz}}{4}\left[I_z^2 - I(I+1)/3 + \frac{\eta}{3}(I_x^2 - I_y^2)\right] - g_n\beta_n \vec{H} \cdot \vec{I}. \quad (1)$$

To reduce the number of unknown parameters in our analysis, we applied a simple crystal-field theory to calculate the magnetic hyperfine coupling $\tilde{A}$ tensor from the g-values observed in an earlier EPR study [6]. This theory has been successfully

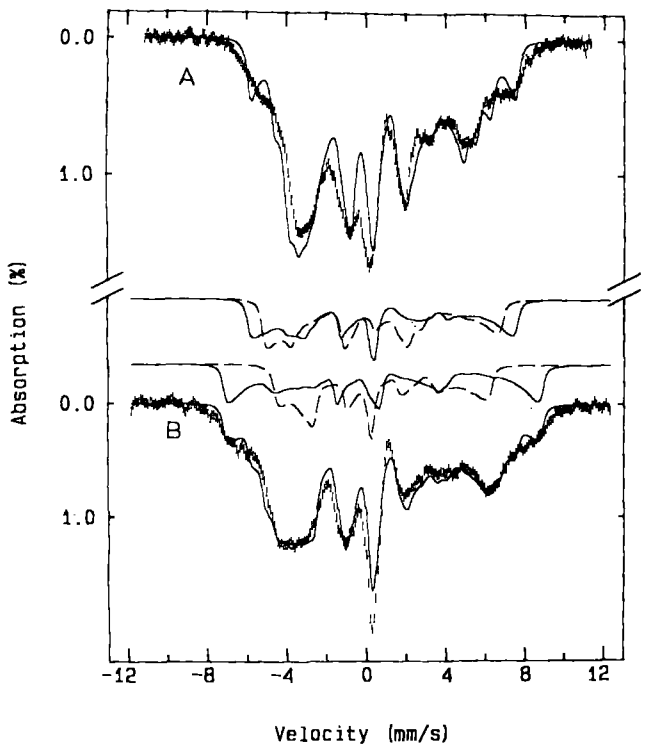

Fig. 2. Mössbauer spectra of the fully oxidized (+ 250 mV) cytochrome c_3 from *D. baculatus* (DSM 1743). The data are recorded at 4.2 K in the presence of a magnetic field of 50 mT (A) and 8 T (B). The fields are applied parallel to the γ-beam. The solid lines plotted over the experimental data are simulations using the parameters listed in Table 1. The individual theoretical spectra corresponding to the four low-spin ferric hemes in a field of 8 T are also shown at the top of spectrum B. Lower traces: (- - - -), for heme 1; (——), for heme 2. Upper traces: (- - - -), for heme 3; (——), for heme 4.

Table 1. Mid-point redox potentials, crystal-field and hyperfine parameters of the low-spin ferric heme groups in cytochrome c_3 from *D. baculatus* (DSM 1743). The numbers in parentheses give the estimated uncertainties in the last significant digits. Δ and v are the axial and rhombic crystal-field parameters, respectively, and λ is the spin-orbit coupling constant. $\eta = (V_{xx}-V_{yy})/V_{zz}$ is the asymmetry parameter, where V_{ii} values are the principal components of the electric field gradient tensor. The magnetic hyperfine A-values are calculated from the listed g-values using a crystal-field theory described in [26]. The mid-point redox potentials and g-values reported without uncertainty are taken from [6].

Parameter	Heme 1	Heme 2	Heme 3	Heme 4
g_x	1.51	1.0 (2)	1.34	1.1 (3)
g_y	2.26	1.84 (15)	2.24	2.16 (20)
g_z	2.93	3.41	3.05	3.18
Δ/λ	3.28	3.80	2.88	2.58
v/λ	1.89	0.96	1.57	1.25
$A_{xx}/g_n\beta_n$ (T)	−40.9	−31.9	−39.3	−37.6
$A_{yy}/g_n\beta_n$ (T)	17.7	17.7	21.2	24.6
$A_{zz}/g_n\beta_n$ (T)	50.4	83.1	58.0	67.3
ΔE_Q (mm/s)	2.0 (3)	2.0 (3)	2.0 (3)	2.0 (3)
δ (mm/s)	0.24 (6)	0.24 (6)	0.24 (6)	0.24 (6)
η	−2.0 (5)	−2.0 (5)	+2.0 (5)	−2.0 (5)
E'_0 (mV)	−70	−280	−300	−355

applied to many studies of low-spin ferric heme compounds [18–24]. Also, in this analysis, the mean ΔE_Q value, 2.0 mm/s, obtained from the high-temperature data is used for all four hemes because the low-temperature magnetic spectra are insensitive to the ΔE_Q values as long as they are within the narrow range indicated by the high-temperature data. Consequently, the only variables in our analysis were the four asymmetry parameters (η) and the g_x and g_y values of hemes 2 and 4 that were not detected in the previous EPR measurements. In this manuscript, the hemes are labelled according to their mid-point redox potentials such that heme 1 has the highest redox potential and heme 4 the lowest.

To deconvolute the magnetic spectra into the four spectral components, we employed a method of spectral differentiation described in a combined Mössbauer and EPR study of a hexaheme cytochrome [25]. This method utilizes Mössbauer spectra of samples poised at different redox potentials. In the following, the procedures for decomposition is briefly outlined. An earlier EPR study [6] indicates that the mid-point redox potential of heme 1, −70 mV, is more than 200 mV higher than those of the other hemes and at −210 mV only heme 1 is reduced while the other three hemes are oxidized. In agreement with this EPR finding, high-temperature Mössbauer measurements of the −210 mV sample shows that approximately 23% of the hemes are reduced. Consequently, difference spectra between those of the +250 mV and −210 mV samples would reveal the spectral component corresponding to the oxidized heme 1. Also, from the EPR study [6], a set of g-values ($g_{max} = 3.05$, $g_{mid} = 2.24$ and $g_{min} = 1.34$) were identified for heme 3. With these known g-values, the crystal-field theory [18, 26] was used to calculate the magnetic hyperfine coupling $\tilde{A}$ tensor and the corresponding Mössbauer spectra for the oxidized heme 3 were simulated. Using these prepared spectral components for hemes 1 and 3, the component for heme 2 was obtained from the difference spectra between those of the +250 mV and the −340 mV samples. The spectral component for heme 4 could then be obtained from the spectra of the +250 mV sample by removing the contributions from hemes 1, 2 and 3. The deconvoluted spectra were then compared with a series of theoretical simulations. This process was repeated until a satisfactory agreement between experiment and theory was obtained.

As mentioned above, the g-values for all four hemes were required for the simulation of the Mössbauer spectra. The three principal g-values for hemes 1 and 3 were determined in the earlier EPR study [6]. For hemes 2 and 4, however, only g_{max} is detected. In order to estimate the other two g-values, we applied the relationship:

$$g_x^2 + g_y^2 + g_z^2 = 16, \qquad (2)$$

which has been shown to be a good approximation for low-spin ferric hemes [27]. The unknown g-values were varied systematically and for each set of variation the corresponding magnetic coupling A-values were calculated, and the Mössbauer spectra were simulated and compared with experiments. A set of parameters which generate theoretical spectra in agreement with experiments is listed in Table 1 and the theoretical simulations are plotted over the data in Fig. 2. The agreement between the simulation and experimental spectra is reasonably good. Theoretical spectra corresponding to each individual heme at 8 T are also plotted in Fig. 2.

DISCUSSION

EPR spectroscopy is commonly applied to the study of low-spin ferric heme compounds. In most cases, a complete

description of the electronic structure (i.e. the electronic energy levels of the iron 3d orbitals) can be inferred from the measured principal g-values [18, 19, 28]. There exist, however, situations where EPR spectroscopy is rather unfavorable and information gathered from another complementary technique is required. For example, in the case of a strong g_{max} value ($g_{max} > 3.3$), only the maximum g-value can be detected and the other g-values are not observable by EPR [29, 30]. Mössbauer spectroscopy, however, has been proven to be very useful in determining the electronic structure of low-spin ferric heme compounds with $g_{max} > 3.3$ [24, 31]. Also, for the studies of multi-heme proteins, there are the added complications of overlapping g-values and of spin-spin interactions which could result in g-values that are completely different from the non-interacting values [25, 32]. Our previous EPR study on *D. baculatus* cytochrome c_3 has identified the principal g-values for both hemes 1 and 3, but detected only the g_{max} values for hemes 2 and 4 [6].

In this manuscript, we continue our characterization study of *D. baculatus* cytochrome c_3 using Mössbauer spectroscopy and have demonstrated that, in conjunction with other complementary techniques, Mössbauer spectroscopy is capable of obtaining detailed electronic structures of the heme iron atoms in proteins containing multiple heme groups. In the reduced *D. baculatus* cytochrome c_3, all four hemes are reduced and exhibit diamagnetic Mössbauer spectra typical for low-spin ferrous ($S = 0$) hemes. In the oxidized cytochrome, the hemes are low-spin ferric ($S = 1/2$) and exhibit magnetic Mössbauer spectra. Even though these magnetic spectra overlap substantially, we were able to deconvolute the raw data of the oxidized protein into four distinct spectral components (corresponding to the four low-spin ferric hemes) through a spectral differentiation method which utilized spectra of samples poised at different redox potentials. Detailed data analysis yielded characteristic parameters describing the distinct electronic structures of the four low-spin ferric hemes. Using this spectroscopic information together with the spectral differentiation method developed in the present study, it is now possible to investigate properties of biochemical significance of each heme group, such as pH dependence and ligand-binding specificity.

It is interesting to note that although the four hemes are of the same type and have the same axial ligands, their mid-point redox potentials are different and range from -355 mV to -70 mV [6]. X-ray crystallographic studies of cytochrome c_3 from *D. vulgaris* (Miyazaki), *D. vulgaris* (Hildenborough) and *D. baculatus* (Norway 4) indicate that the four hemes are situated in different protein environments and that the orientations of their axial ligands are different [2–5]. This difference in environment and structure are believed to have a strong influence in controlling the mid-point redox potentials of the hemes. Our present study indicates that the detailed electronic structures of the hemes are different, which obviously must also be reflecting the environmental and structural differences. It is therefore important to examine whether a direct correlation exists between electronic structure and redox potential, and thereby to provide a mechanism in relating spectroscopic data to thermodynamic properties. Research along this line of investigation is currently underway.

This work is supported by the National Institutes of Health grants GM 414821 (JJGM and JLG) and GM 32187 (BHH), the National Science Foundation grant DMB 9001530 (BHH) and grants (IM and JJGM) from *Junta National de Investigação Cientifica e Tecnológica* and from *Instituto Nacional de Investigação Cientifica*.

REFERENCES

1. Yagi, T., Inokuchi, H. & Kimura, K. (1983) *Acc. Chem. Res. 16*, 2–7.
2. Higushi, Y., Kusanaki, M., Matsuura, Y., Yasuoka, N. & Kakudo, M. (1984) *J. Mol. Biol. 172*, 109–139.
3. Haser, R., Pierrot, M., Frey, M., Payan, F., Astier, J. P., Bruschi, M. & LeGall, J. (1979) *Nature 282*, 806–810.
4. Pierrot, M., Haser, R., Frey, M., Payan, F. & Astier, J. P. (1982) *J. Biol. Chem. 257*, 14341–14348.
5. Kissinger, C. R. (1989) *Ph. D. Thesis*, University of Washington, Seattle, Washington, USA.
6. Moura, I., Teixeira, M., Huynh, B. H., LeGall, J. & Moura, J. J. G. (1988) *Eur. J. Biochem. 176*, 365–369.
7. Gayda, J. P., Benosman, H., Bertrand, P., More, C. & Asso, M. (1988) *Eur. J. Biochem. 177*, 199–206.
8. Gayda, J. P., Bertrand, P., More, C., Guerlesquin, F. & Bruschi, M. (1985) *Biochim. Biophys. Acta 829*, 262–267.
9. Gayda, J. P., Yagi, T., Bensman, H. & Bertrand, P. (1987) *FEBS Lett. 217*, 57–61.
10. Cammack, R., Fauque, G., Moura, J. J. G. & LeGall, J. (1984) *Biochim. Biophys. Acta 784*, 68–74.
11. Santos, H., Moura, J. J. G., Moura, I., LeGall, J. & Xavier, A. V. (1984) *Eur. J. Biochem. 141*, 283–296.
12. Moura, J. J. G., Santos, M. H., Moura, I., LeGall, J., Moore, G. R., William, R. J. P. & Xavier, A. V. (1982) *Eur. J. Biochem. 127*, 151–155.
13. Fan, K., Akutuso, H., Kyogoku, Y. & Niki, K. (1990) *Biochemistry 29*, 2257–2263.
14. Park, J.-S., Kano, K., Niki, K. & Akutsu, H. (1991) *FEBS Lett. 285*, 149–151.
15. Huynh, B. H., Czechowski, M. H., Krüger, H. J., DerVartanian, D. V., Peck, H. D. Jr & LeGall, J. (1984) *Proc. Natl Acad. Sci. USA 81*, 3728–3732.
16. Fauque, G. (1985) *These de Doctorat d'Etad*, Université de Tecnologie, Compiègne, France.
17. Dutton, P. L. (1978) *Methods Enzymol. 54*, 411–435.
18. Griffith, J. S. (1971) *Mol. Phys. 21*, 135–139.
19. Taylor, C. P. S. (1977) *Biochim. Biophys. Acta 491*, 137–149.
20. Brautigan, D. L., Feinberg, B. A., Hoffman, B. M., Margoliash, E., Peisach, J. & Blumberg, W. E. (1977) *J. Biol. Chem. 252*, 574–582.
21. Huynh, B. H., Emptage, M. H. & Münck, E. (1978) *Biochim. Biophys. Acta 534*, 295–306.
22. Rhynard, D., Lang, G., Spartalian, K. & Yonetani, T. (1979) *J. Chem. Phys. 71*, 3715–3721.
23. Dwivedi, A., Toscano, W. A. Jr & Debrunner, P. G. (1979) *Biochim. Biophys. Acta 576*, 502–508.
24. Walker, F. A., Huynh, B. H., Scheidt, W. R. & Osvath, S. R. (1986) *J. Am. Chem. Soc. 108*, 5288–5297.
25. Costa, C., Moura, J. J. G., Moura, I., Liu, M. Y., Peck, H. D. Jr, LeGall, J., Wang, Y. & Huynh, B. H. (1990) *J. Biol. Chem. 265*, 14382–14387.
26. Oosterhuis, W. T. & Lang, G. (1969) *Phys. Rev. 178*, 439–456.
27. De Vries, S. & Albracht, S. P. J. (1979) *Biochim. Biophys. Acta 546*, 334–340.
28. Peisach, J., Blumberg, W. E. & Adler, A. (1973) *Ann. N. Y. Acad. Sci. 206*, 310–327.
29. Salerno, J. C. (1984) *J. Biol. Chem. 259*, 2331–2336.
30. Gadsby, P. M. A. & Thomson, A. J. (1986) *FEBS Lett. 197*, 253–257.
31. Huynh, B. H., Lui, M. C., Moura, J. J. G., Moura, I., Ljungdahl, P. O., Münck, E., Payne, W. J., Peck, H. D. Jr, DerVartanian, D. V. & LeGall, J. (1982) *J. Biol. Chem. 257*, 9576–9581.
32. Anderson, K. K., Lipscomb, J. D., Valentine, M., Münck, E. & Hooper, A. B. (1986) *J. Biol. Chem. 261*, 1126–1138.